Support point determination for support structure design in additive manufacturing

Zhiping Wang, Yicha Zhang, Shujie Tan, Liping Ding, Alain Bernard

Version of Record: https://www.sciencedirect.com/science/article/pii/S2214860421004991
Manuscript_b4f60badfa019a8a9208fa21e3e56761

Support Point Determination for Support Structure Design in Additive Manufacturing

[a]Zhiping Wang, [b]Yicha Zhang*, [c]Shujie Tan, [c]Liping Ding, [a]Alain Bernard

[a]*Ecole Centrale de Nantes, LS2N, CNRS UMR 6004, Nantes, France*
[b]*UTBM – Université de Technologie Belfort-Montbéliard, ICB-COMM, CNRS UMR 6303, Sevenans, France*
[c]*College of Mechanical & Electrical Engineering, Nanjing University of Aeronautics and Astronautics, Nanjing, China*

*Corresponding author. E-mail address: yicha.zhang@utbm.fr (Y. Zhang)

Abstract

Support structures are necessary for many AM (additive manufacturing) processes to maintain the overhanging areas or resist deformation caused by thermal stress in printing. The design of support structures affects not only the printing quality but also material consumption and post-processing time. Current research had proposed many support structure designs and optimization methods to meet varying optimization requirements. However, no research has investigated yet how to determine the support points, or contact points for optimal support design. The number and position of support points will directly affect the support structure's performance and volume, and therefore the final printing quality. To fill this gap, this paper proposes a determination method, which integrates overhang detection, analysis of periodic support point patterns and AM constraints to optimize support point distribution with ensured manufacturability. It is particularly critical for complex and porous structures in medical applications. The proposed method is illustrated and validated through a complex dental component. It can be used with support structure design methods to further improve the support structure performance and reduce support volume in printing, especially for metallic AM processes.

Keywords: Support point optimization; Support structure design; Additive manufacturing.

1. Introduction

AM (additive manufacturing) has many benefits for complex and highly customized component fabrication due to its non-linear cost-complexity relationship [1-3]. It has become a competitive processing method to manufacture customized high-value components for medical and aeronautic applications. However, there are a few difficult decision-making problems along the AM digital processing chain. In the preparation stage, a set of preparation tasks, e.g. build orientation determination [4, 5], support structure design [6], slicing and scan path planning [7], have a direct impact on the printing results. Among these tasks, support structure design and optimization is crucial for saving raw materials, improving support performance and reducing post-processing time, especially in the powder bed based metallic AM processes, e.g. SLM (selective laser melting). The support structures not only sustain the overhang areas and concave features, e.g. holes and curved bridges of a component in printing, but also act as heat diffusion mediums and thermal distortion resisting structure [8, 9]. Therefore, it becomes a core research question to design support structures with lightweight, easy-to-remove characteristics for post-processing and friendly heat-diffusion properties.

Support structure design is one of the inevitable preparation tasks in many metal AM processes. Generally, there are four main functions of support structures: to support overhang areas, holes or bridges for printability; to maintain part manufacturability during printing; to enable easy removal from the build base ; to assist heat diffusion or resist residual stresses in a dynamic thermal field caused by laser melting in scanning [10]. The strategies of support structure design and optimization usually have two categories: direct and indirect. Direct methods mean direct design and optimization for a given fixed design and build orientation, while indirect methods indicate the adaptation or redesign of a component, e.g. shape adaptation of overhang area or geometric features. Both direct and indirect methods always aim to minimize the volume of support, achieve easy post-processing with an acceptable printing quality of the component and

support heat transfer to reduce thermal stress impact. To generate support structures for a component with a given build orientation, there are two main steps: 1. To identify overhang areas and 2. To generate support volume topologies to connect the identified areas with the build base. To identify the overhang areas, the geometric facet information and the component slices are usually used as inputs. Then, AM manufacturing constraints, e.g. maximum lateral bridge printing length and maximum available inclination angle, are used to help determine the areas to connect supports.

Direct methods, used by many commercial AM preparation tools, focus on generating uniformed but simple shape support structures in the projection region since it can be easily manipulated. For the direct projection-based methods, evenly distributed support points are projected from the build base onto the overhang areas, then linear support structures with predefined cross-section profiles are generated along the projection direction. With the aim to reduce support volume for saving raw materials, in recent years more lightweight support structure generation methods have been proposed, such as cellular filling structures and tree-shaped structures. Fig .1 gives a brief literature review of main representative lattice and tree-shaped support structure generation methods, especially for SLM process. For the cellular filling methods, predefined lattice support structures were proposed in [6, 9, 11]. Lattice cells were mapped to replace solid bars or walls in the projection method to form lattice supports to reduce the volume of support materials. To explore more filling unit cells, three new types of filling cell shapes were applied in [12]. However, there is still too much material used for the supports. To increase material reduction, Dijkstra's algorithm [13] was used to find the shortest connection path from the initial projection area which was fully filled with lattice units. Considering the manufacturability in practice, a new verified lattice cell method [14] was used to fill the support volume projection space as an initial structure, and then a genetic algorithm (GA) was applied to search for a shortest lattice bar path within the initial lattice filling structure by removing a maximum number of lattice beams and obtaining tree-shaped support structures. Compared with a tree-like support structure method in Meshmixer [15], a more effective tree-like support method was introduced to support the overhang areas in [16]. To explore more types of tree-shape structures, a modified local tree node generation rule based on supporting cone was reported in [17]. Similarly, by constructing a grid in the support projection space for populating tree nodes, advanced searching algorithms were applied to obtain the shortest accumulative path length to form lightweight tree support structures [18, 19]. In addition, in [20], a horizontal bridge support structure design method was introduced to simplify the support structure generation procedure. The maximum bridge length was tested and taken into consideration in the support structure design. More recently, a bio-inspired design method was proposed to design and optimize lightweight but qualified support structures [21]. A generative design method and printing simulation were used to populate and select self-support structures. Support point determination was firstly mentioned and implemented by a simple optimization algorithm. But, in this work, the optimization is limited to prefixed support point distribution pattern without analysis and simplification of support areas (overhanging areas).

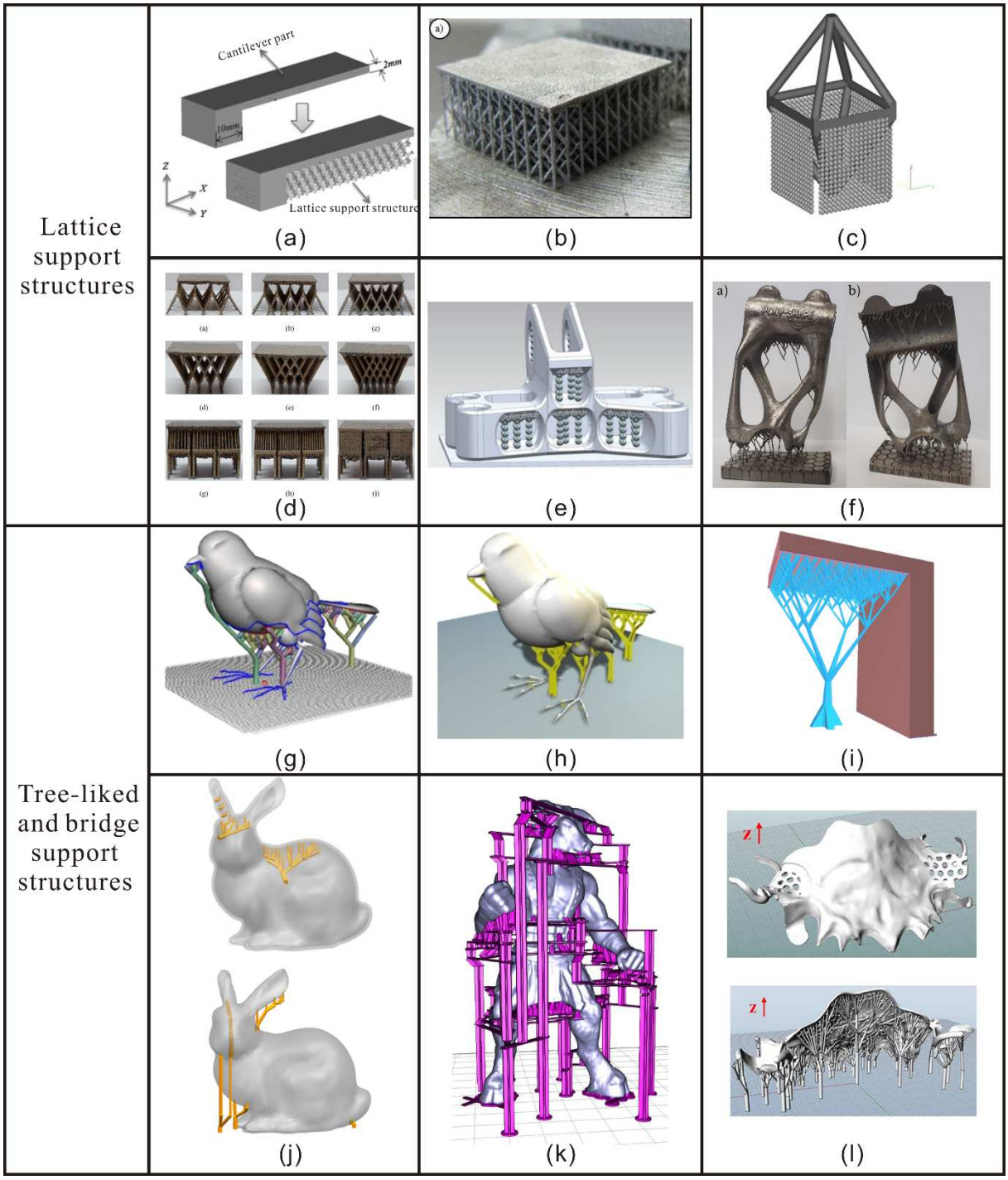

Fig. 1. Main representative methods of lattice and tree-shaped support structure generation: (a). a TPMS-based lattice support structure-1 [6]; (b). a strut-based lattice support structure-1 [9]; (c). a TPMS-based lattice support structure-2 [11]; (d). a strut-based lattice support structure-2 [12]; (e). a lattice support with hollow unit cells in the interface [13]; (f). a pruned strut-based lattice support structure [14]; (g). a tree-shaped support structure-Meshmixer [15]; (h). a tree-shaped support: Clever support [16]; (i). a tree-shaped support structure-1 [17]; (j). an internal and external tree-shaped support structure [18, 19]; (k). a bridge support structure [20]; (l). a bio-inspired tree support structure [21].

2. Current research problem

According to the research works above, many existing solutions for support structure methods are still limited to simple metallic components with less complex fine surfaces or holes and can hardly meet the requirements from real applications, like the complex components from medical applications as illustrated in Fig. 2. On the other hand, even though current commercial support software, such as e-Stage from Materialise [22] and Netfabb from Autodesk [23], can provide a stable and multifunctional support, the corresponding support areas are usually massive since overhang areas are not analyzed and optimized further. The situation will get worse when a large number of complex freeform and porous overhang areas

exist in Fig. 2, where there are many fine critical features in the inner surface of a dental part. For these kinds of components, it is hard to detect the reasonable overhang regions and determine the corresponding optimal support points. Although the research works discussed above had made so many efforts in the support structure optimization, most of them ignored how to simplify the original overhang areas, and paid no attention to the determination of an optimal support point distribution (optimal number and locations) on the simplified overhang areas. In addition, most papers in literature only used demonstration STL (STereoLithography) model examples with quite simple regular shapes, e.g. flat overhang surfaces, as overhang regions, which are easy for support design and generation. However, the applicability of many reported methods in literature is not clear for real industrial and medical cases.

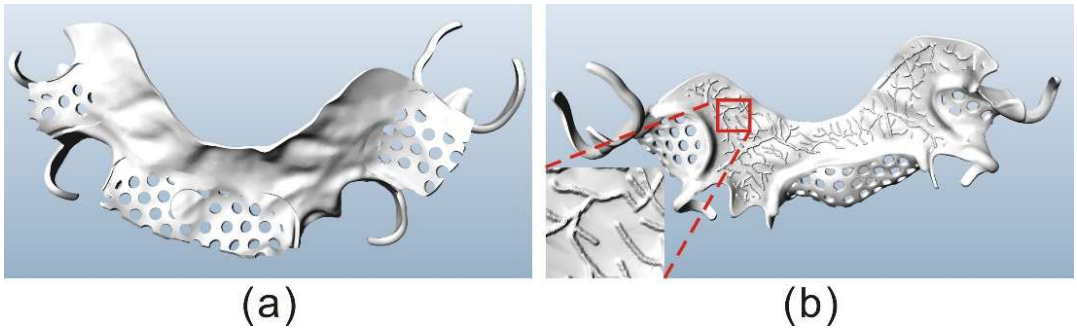

Fig. 2. A medical component STL model: (a). the outer surface of a dental part; (b). fine critical features of the dental part.

Generally, current overhang determination method mainly utilizes the critical overhang angle to identify the overhang areas, called original overhang areas in this paper. However, with the consideration of other AM constraints, maximum overhang distance and minimum feature size, the overhang areas can be further simplified and optimized to obtain valid overhang areas that must be supported, called support relevant overhang areas in this paper. Fig. 3 uses a smaller dashed box to represent the practice of existing methods in literature and shows the expected extension to make for support relevant overhang determination.

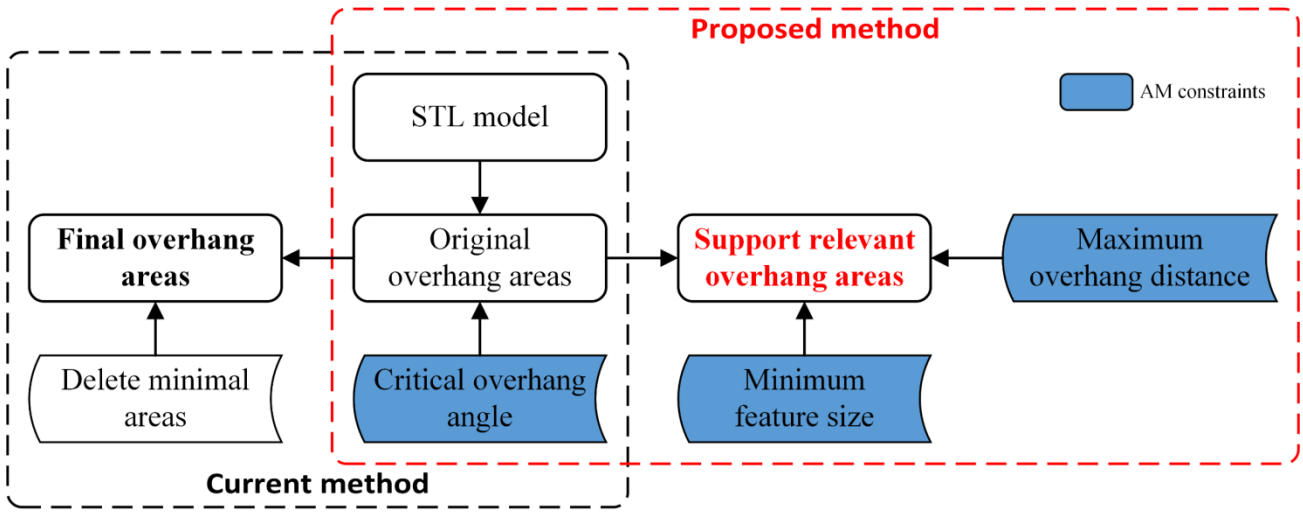

Fig. 3. Extension to determine support relevant areas with more consideration of AM constraints.

For commercial software tools, such as Magics and Netfabb, final overhang areas are determined by deleting minimal overhang areas. Fig. 4(a, b) presents two lattice support structures with different minimal area thresholds from Netfabb as an example. Since the dental part has many small fine overhang areas, it is hard to ensure the part printing quality only by supporting overhang areas bigger than the minimal area threshold. With a lower minimal area threshold, more support points are selected, as illustrated in Fig. 4(c, d). However, small overhang areas are close to each other, hence the selection of support points is very dense while defining a lower minimal area threshold. Fig. 4(e, f) can show the support points more clearly. Therefore, one of the most serious problems in current commercial software tools is that part of overhang areas needing to be supported are abandoned due to their small size. As shown in Fig. 4(g, h), the overhang areas marked

should be supported. Since the features are less than the minimal area, they are usually ignored while a higher threshold is set. Generally, these overhang areas need to be selected manually. This will require experienced engineers to involve into support decision-making and arouse the repeatability or stability problem for printing quality. Therefore, it is a barrier for the industrialization of AM process, especially not suitable for mass production in the dental field.

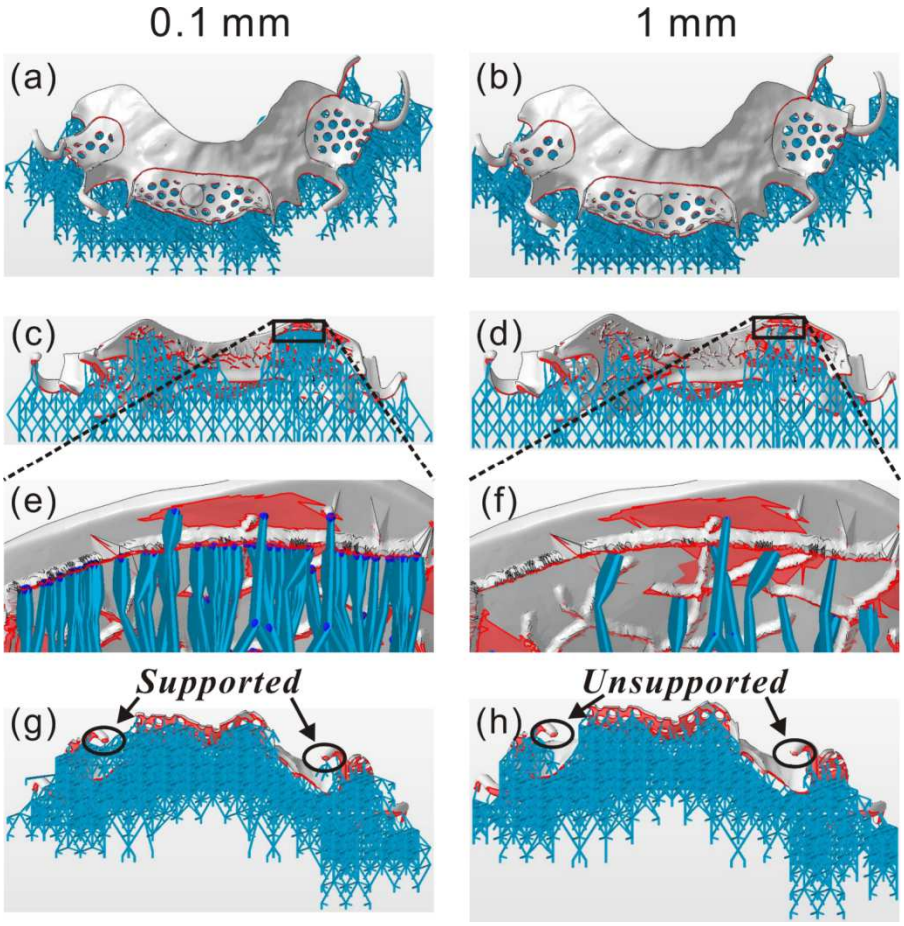

Fig. 4. Threshold value setting caused difference of support structure and stability problem in Netfabb.

In summary, the key steps and related complexity to determine support relevant overhang areas and optimal support point distribution had not yet been thoroughly discussed. Furthermore, there is no research to investigate the generation sequence of support points to assign in different locations of a component with a predefined build orientation. To fill this gap, this paper proposes a support point determination method with an objective to be used as inputs for many different support design methods. It at first addresses how to detect and select reasonable support relevant overhang regions in an optimal way taking into consideration more AM constraints and application requirements. Meanwhile, a sequential strategy of support point generation is proposed to assist support point optimization on the selected support regions. Then, a new support point pattern is developed so that the redundancy of current support point distribution is alleviated. To obtain an optimal support point set, a GA optimization method is applied to optimize the number and position of support points on support relevant overhang areas. As expected, the proposed method can help decrease the number of unnecessary support points on the overhang areas significantly, thereby reducing the support volume and the post-processing time while ensuring manufacturability, which means a stable support function to ensure the printing quality, e.g. shape accuracy and surface quality. The following sections will introduce the method modules and their technical implementations. A case study is presented at the end to demonstrate the method.

3. Global view of the proposed method

In the preparation stage of AM, build orientation determination has a direct effect on support structure design, especially for complex components. The determination of build orientation coupled with the support

structure design is essential since it directly defines the solution space of the support structure design problem. To limit the scope of this research, the proposed method starts with a given build orientation. With regard to the build orientation optimization problem for medical components, a statistical build orientation determination method can be found in [24]. Fig. 5 below describes the general method workflow.

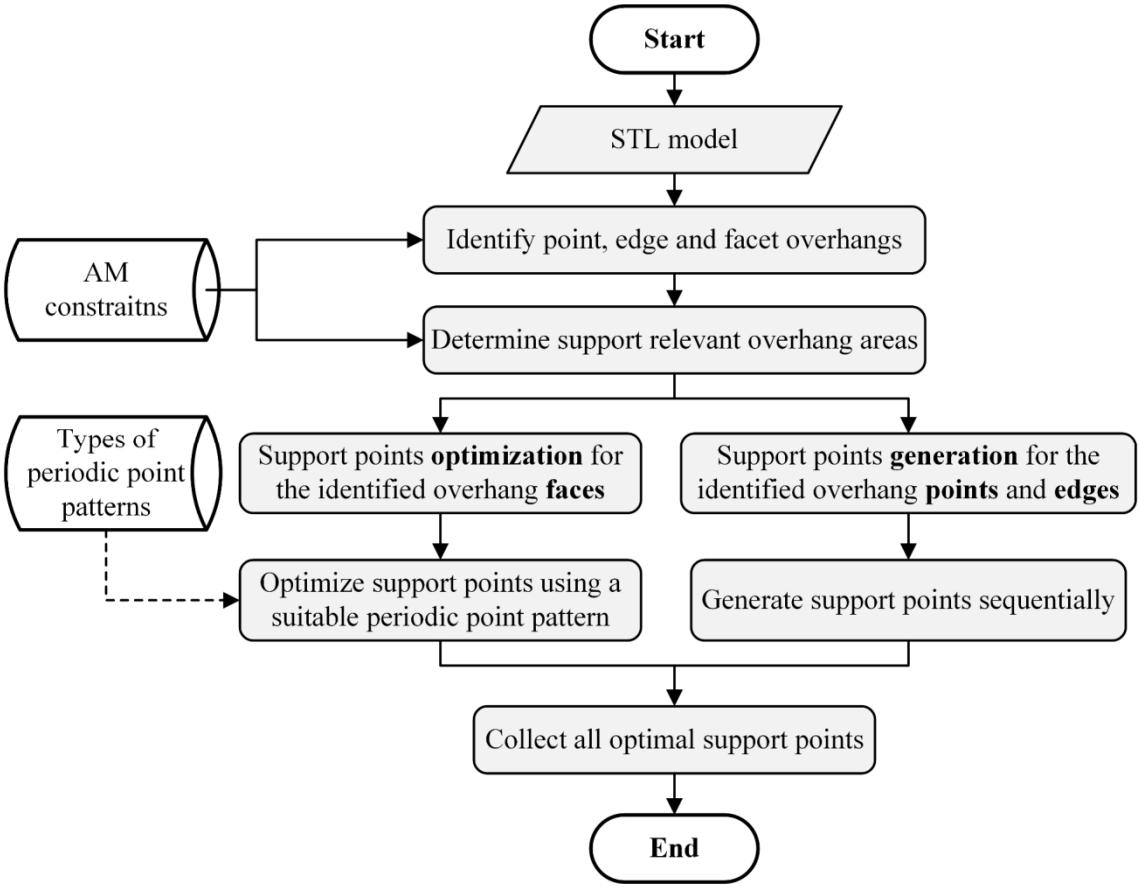

Fig. 5. Workflow of the support point generation & optimization method.

The input to the methodology is an STL model represented by a boundary mesh with a predefined build orientation. Then, the following key step is to identify three types of overhang areas, including points, edges and faces. Facet geometric information and specific AM manufacturing constraints are used to detect and classify the support areas. This step of the proposed method is unique and different from that reported in research literature. After this, the next critical step is the application of a combined optimization method for support point optimization for the three main types of support areas: overhang face, overhang edge and overhang isolated tip point, separately. An optimal periodic support point pattern is defined and used for face overhangs while a special support point generation scheme is applied to edge and tip point overhang types to sequentially identify the valid support points. Finally, all the generated support points are combined to a support point set for the whole STL model in a pre-defined build orientation. The details of the two main modules of the proposed method are presented in the next two sections.

4. Analysis of support relevant overhang areas

If there is no underlying layer to support overhang areas, a structure will deform or even collapse, especially for the powder-based fusion process. Facet geometric information and AM constraints are usually employed to help identify overhang areas. Regarding an overhang region, overhang features can usually be divided into face overhang, edge overhang and point overhang [16, 25] as shown in Fig. 6.

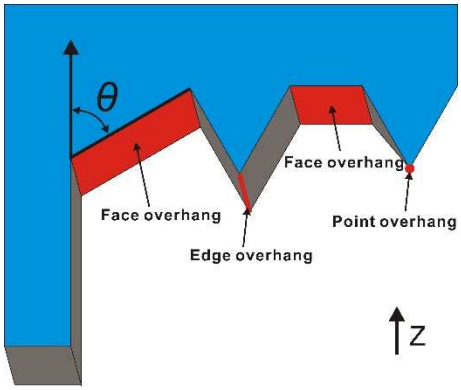

Fig. 6. Illustration of point, edge and face overhangs.

Since the overhangs are different, the way to determine support points may be different. For isolated overhang points, they should be seen as support points directly. However, support point generation and optimization on or near overhang edges and faces should be discussed separately and treated differently. Three types of overhangs can be determined by geometric information of mesh models and corresponding AM process constraints, e.g. maximum overhang length and angle. More detailed definitions for these overhang types are explained and discussed below.

- A point overhang is a point that is located lower than all other points in neighboring meshes on condition that the angle θ between the normal vector of an adjacent mesh (at least one) and the printing direction Z is bigger than 90°. Fig. 7(a) and (b) describe two types of overhang points and Fig. 7(c) shows a non-overhang point where all normal vectors are not facing the base.
- An edge overhang is considered as an overhang if other edges of the two incident faces are located higher with at least one normal vector of the two incident faces facing the building base. Edge overhang is determined similarly to that for the point overhang. Fig. 7(a) and (b) can also be seen as section views of two edge overhangs.
- A mesh face is defined as a downward overhang face if the angle, θ, between the mesh face plane and the printing direction vector Z is bigger than the printable overhang angle.

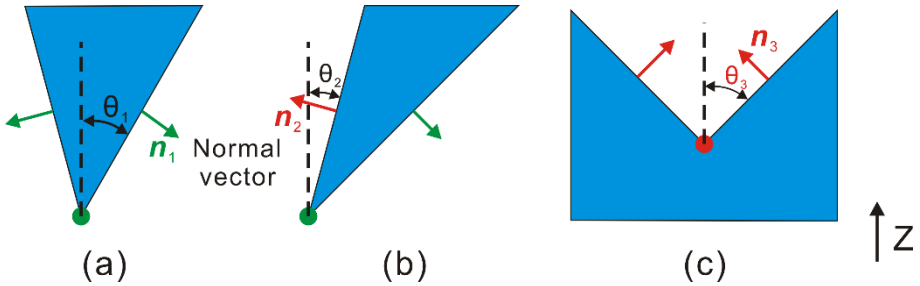

Fig. 7. Illustration of overhang points identification (overhang points marked in green). (a). overhang point: all incident faces are facing the base; (b). overhang point: at least one normal vector of the adjacent meshes is facing the base; (c). non-overhang point: all normal vectors of the incident faces are not facing the base.

4.1. Support relevant overhang areas

Geometric information can help to detect all the overhang types. However, not all of them need support or require support point assignment since the manufacturability of AM processes can further help filter the detected overhangs to reduce the support volume in the end. The filtered overhangs, which need to be supported, are regarded as support relevant overhangs in this research.

Support relevant overhang points

After detecting all overhang points, support relevant overhang points that must be supported need to be discovered. Fig. 8 gives an illustration of filtering by finding the nearest non-supported points on an active

plane that is parallel to the building base. The non-supported points should be located on mesh faces that do not contain any types of overhang areas. In other words, the non-supported points are intersection points between the active plane (parallel with the build base plane) and non-overhang areas (point ***N*** in Fig. 8) that does not include overhang points and edges. Usually the principle of judging whether an overhang point needs support is whether distance *D* between the overhang point and the nearest non-supported point in the active plane is less than the maximum overhang distance. However, the maximum overhang distance is suitable for evaluating the position of support points on the overhang faces. Due to the islanding characteristic of the overhang points on the active plane, it is undesirable to use a maximum overhang distance to detect whether an overhang point needs to be supported. Here, the minimum feature size for the AM process is used to help judge whether an overhang point needs support. If distance *D* is more than the minimum feature size, the feature point cannot be printed under the premise of ensuring the feature. Hence, the overhang points identified are defined as support relevant overhang points here.

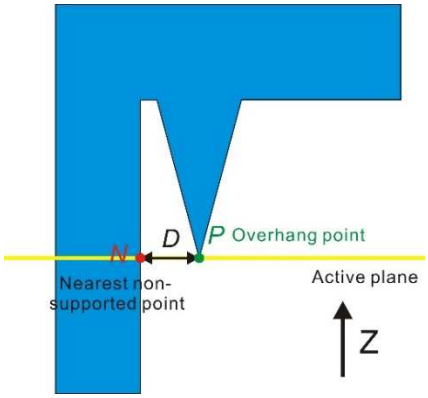

Fig. 8. Illustration of a support relevant overhang point identification (Point *N* is the non-supported point closest to the overhang point (*P*). Distance (*D*) is the distance between *N* and *P*. *Z* is the printing direction).

Support relevant overhang edges

For cases of isolated overhang edges, the edges are broken down into overhang points by active planes (yellow lines in Fig. 9). The lower endpoint of each overhang edge is seen as a decomposition point. When the length of an overhang edge projected onto the XOY plane is less than the maximum bridge length, the decomposition point is the lower endpoint. If the projected length is more than the critical length, the edge is divided into several segments which are shorter than the critical length. These active planes parallel to the XOY plane pass through the decomposition points of overhang edges. Fig. 9(a) shows the example of overhang edges decomposed into several overhang points. With reference to Fig. 8, the discussion is whether these decomposition points of overhang edges need support. For those points that need support, the overhang edges containing these points are considered as support relevant overhang edges. With regards to the support relevant overhang edges that must be supported, they are projected as polylines onto the XOY plane. The sequence of generating projected support points for these support relevant overhang edges is determined as shown in Fig. 9(b). Due to the bottom-up printing characteristics, local and global lowest points on the overhang edges should be supported first. Hence, the local and global lowest points of these support relevant overhang edges are found to generate projected support points preferentially. The generation sequence of projected support points should be derived from the global point along both sides of the edges until covering all overhang edges. The series of numbers indicate a generation sequence of the projected support points.

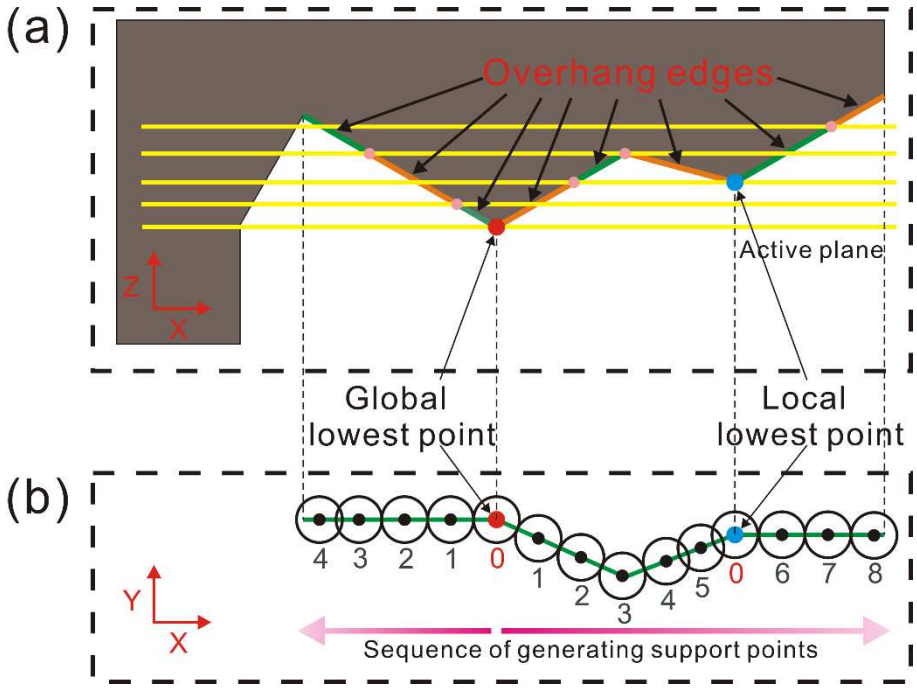

Fig. 9. Support point generating on support relevant overhang edges: (a). these edges on XOZ plane (red and blue points are the global and local lowest points on the support relevant overhang edges, respectively); (b). generation sequence of support points projected on the XOY plane.

Support relevant overhang faces

In terms of continuous overhang faces in Fig. 10(a, b), the projection of the overhang faces is extracted in Fig. 10(c). Boundary meshes and their corresponding adjacent non-overhang meshes are identified using mesh geometric information illustrated in Fig. 10(d, e). Since the intersecting boundary between the overhang faces and lower neighboring non-overhang areas can provide support within the maximum printing bridge length, the boundary of the lower non-overhang meshes (Fig. 10(f)) is obtained as shown in Fig. 10(g). Each edge of the neighboring non-overhang mesh faces has a support region in Fig. 10(h). To clarify the support area of a non-supported edge, Fig. 10(i) presents an enlarged support area that an edge can cover. *r* indicates the maximum printing bridge length. To obtain the overhang faces that need support, the support region is removed from the original overhang faces. Hence, the filtered or identified overhang area, called support relevant overhang area, is finally shown in Fig. 10(j, k).

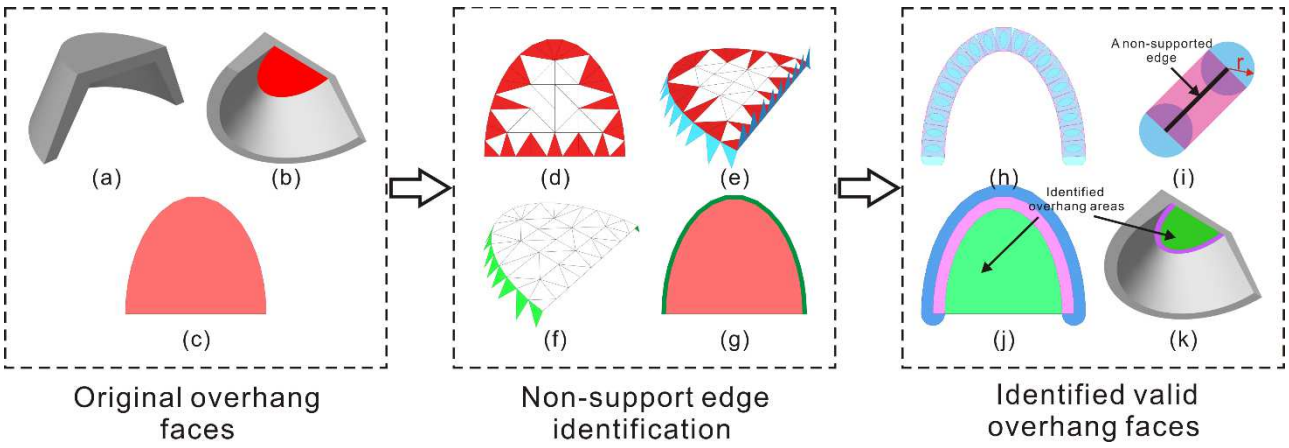

Fig. 10. Illustration of support relevant overhang faces area. (a). a STL model; (b). original overhang faces; (c). projection of the overhang area onto the XOY plane; (d). boundary meshes of the original overhang faces; (e). neighboring non-overhang meshes (blue) at the edge of the original overhang faces; (f). identified neighboring meshes that can support the edge of the original overhang face; (g). intersecting curve (green) between identified neighboring mesh and the original overhang faces; (h). support areas that intersect edges between the neighboring non-overhang mesh and the face overhang can play a support role; (i). a cover area that a non-supported edge can support; (j, k). final support relevant overhang area in green and non-supporting overhang area in pink.

4.2. Classification for different types of support relevant overhang areas

Since the way of support point generation is different for these three types of overhang regions, a classification method is proposed to facilitate the analysis of support points. Generally, isolated overhang points can be considered as support points. With regard to overhang edges with overhang points, the overhang points should firstly be marked as support points, and then support point generation method for overhang edges is applied to generate support points. For overhang faces, overhang points and edges on the overhang faces should be analyzed and identified first as predefined support points. Then, a support point pattern should be applied to the overhang faces. By considering the geometry relationship of the three overhang types, three overhang sets are defined in Table 1. These overhangs on the same set should be analyzed together to help generate and optimize support point distribution. In *Set 1*, overhang points, O_{p1}, that are not located on the overhang edges and faces are classified as isolated overhang points. This type of independent or isolated overhang points needs to be supported separately. In *Set 2*, overhang points that are on the overhang edges and not on the overhang faces, O_{p2}, and overhang edges that are not on the overhang faces, O_{e1}, are combined to analyze the generation sequence of support points on the overhang areas as illustrated in Fig. 9. In terms of overhang faces that contain overhang points and edges, support points on the overhang points and edges are generated first. These support points are then defined as predefined support points.

Table 1. The definition of overhang sets based on a classification of support relevant overhang regions.

Types of overhangs	Set	Definition
Support relevant overhang points	*Set 1*	O_{p1}: points that are not on the overhang edges and faces (isolated overhang points)
	Set 2	O_{p2}: points that are on the overhang edges and not on the overhang faces.
	Set 3	O_{p3}: points that are only on the overhang faces.
Support relevant overhang edges	*Set 2*	O_{e1}: edges that are not on the overhang faces (isolated overhang edges)
	Set 3	O_{e2}: edges that are on the overhang faces
Support relevant overhang faces	*Set 3*	O_f: all faces

In the next step the support areas, covered by these predefined support points, are removed to the overhang faces. These overhang faces with holes are called porous overhang faces/areas. Fig. 11 gives an illustration to show the transition from a non-porous overhang area to a porous overhang area. Once the identification and classification of the overhang areas are finished, support point generation and optimization should be conducted to generate optimal numbers and positions for the three types of support relevant overhang sets. In the next section, a new support point pattern and its optimal generation method are introduced. Then, the non-porous and porous overhang areas are defined and the corresponding support point optimization methods for the two types of overhang areas are introduced, especially for the porous overhang faces.

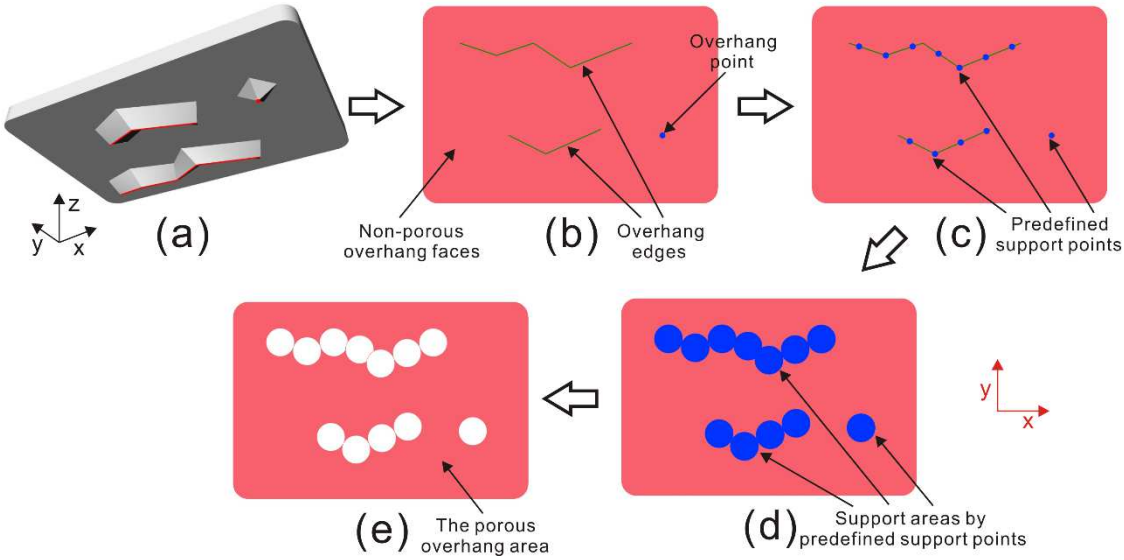

Fig. 11. A transition from a non-porous overhang face to a porous overhang face: (a). overhang point and edges on overhang faces; (b). projection area of the three types of overhang areas; (c). predefined support points on the overhang point and edges; (d). support areas supported by the predefined support points; (e). the porous overhang face.

5. Support point optimization

In this section, a support point optimization method is proposed to optimize support point distribution on support relevant overhang areas. The proposed approach is divided into two main steps. The first is to select a type of predefined periodic point pattern. The second step is to apply the selected periodic support point pattern and an optimization algorithm to optimize support point distribution. Here, a periodic point distribution is used to describe a support point pattern that repeats itself with a specific periodic rule in a given generation sequence. A square periodic point pattern is applied in most existing studies. Here, more kinds of support point patterns are analyzed to search for a better support point distribution.

5.1. Determination of periodic support point pattern

Before analyzing the periodic support point pattern, the maximum bridging length of AM process is applied to determine the radius of nearby areas that a support point can support. In other words, a support point can support an overhang area projected as a circle onto the XOY plane, the radius of which is the maximum printing bridge length of AM capability. Fig. 12 shows two examples to describe the effect of unsupported bridges and horizontal holes without a support structure. As the distance of the unsupported overhang area increases in Fig. 12(a), it shows a poor quality on the downward facing surfaces [26]. Hence, holes below a certain size can be printed without supports. In Fig. 12(b), holes with a diameter of less than 8 mm can be self-support. Hence, a small overhang can be printed when the size of bridges or holes is less than a critical overhang distance.

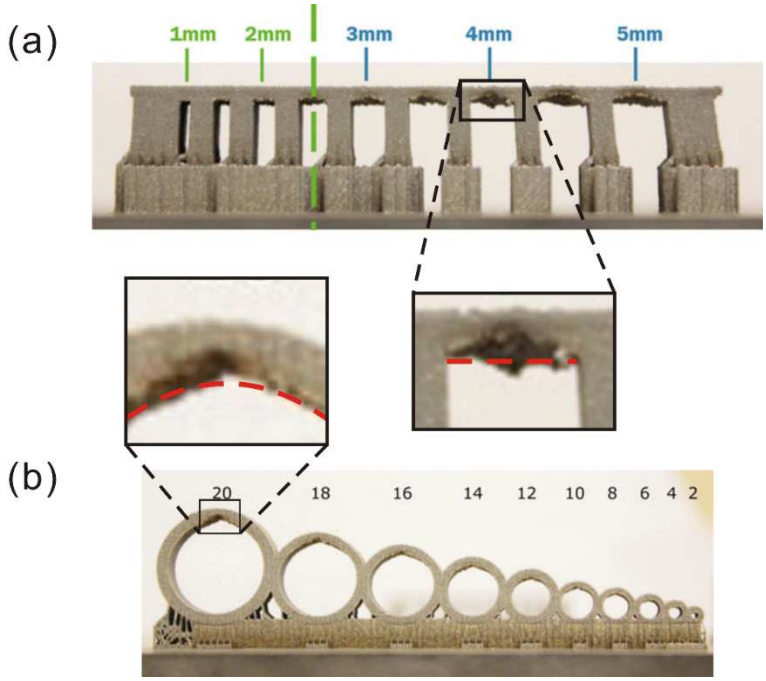

Fig. 12. The maximum printing bridge length of AM capability: (a). effect of unsupported bridge for the powder bed fusion process [26]; (b). horizontal holes printed without support structure [26].

Generally speaking, more support points on the overhang areas means more support structures for a certain overhang area. In tree-like or lattice supporting structures, a periodic support point pattern with square uniform sampling, as shown in Fig. 13(1-3), had been widely used in support structure design. In terms of geometry characteristics, periodic support point patterns in Fig. 13(a) and (b) have the same distribution type. To enlarge the solution space for optimization, more patterns, represented by regular polygons, are discussed in the following.

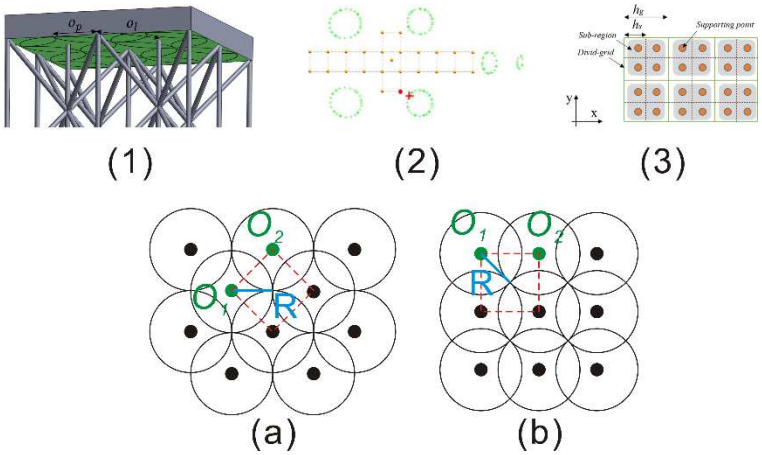

Fig. 13. Periodic support point patterns: (a). supporting points on the overhang areas for lattice support structure in (1) [14]; (b). the sampling support points on the overhang regions for tree-like support structure in (2) and (3) [17, 19].

With regard to a simple regular n-gon $(n \geq 3)$ in Fig. 14(a), the sum of all the internal radians is $(n-2)\pi$. Hence, the internal angle of regular n-gon is $\alpha = (n-2)\pi/n$. The circumradius R from the center of the regular polygon to one of the vertices is related to the side length L. The equation is written as:

$$L = 2R\sin\frac{\theta}{2}\left(\theta = \frac{2\pi}{n}\right) \tag{1}$$

To avoid excessive support overlapping (blue area in Fig. 14(b)) between the support regions defined by two adjacent vertices, the size relationship between the side length L of a regular polygon and the circumradius R should be constrained as:

$$R \le L \le 2R \tag{2}$$

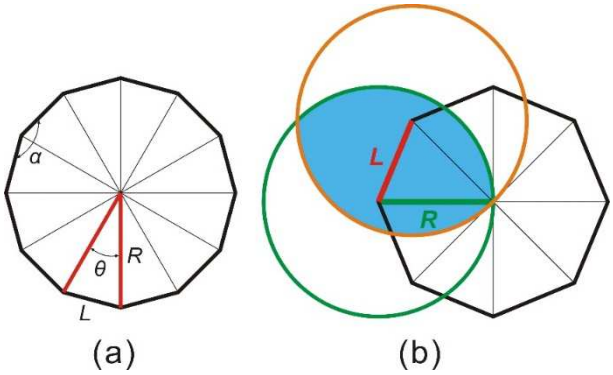

Fig. 14. Regular *n*-gon with side length *L*, circumradius *R*.

From equation 1 and inequality 2, the number of sides n should be constrained as: $\frac{6}{5} \le n \le 6$. Considering $n \ge 3$, n should be $3 \le n \le 6 (n \in N^+)$ or $n = 3,4,5,6$. Fig. 15 provides the four kinds of periodic support point patterns of regular polygons.

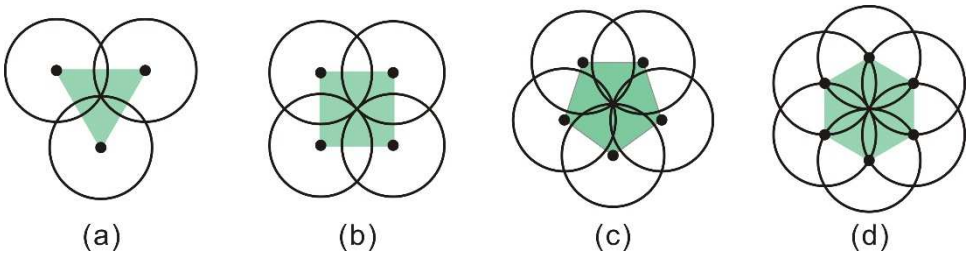

Fig. 15. Periodic support point patterns of regular polygons: (a). side = 3; (b). side = 4; (c). side = 5; (d). side = 6.

To analyze support areas for the four patterns, Fig. 16 gives the four types of multi-group regular polygon patterns. In order to avoid the overlapping situation (Fig. 16(c)), the number of regular polygons for specific multi-group support point patterns, noted a in formula (3), is suggested to be integer. The equation can be written as:

$$a = \frac{2\pi}{\alpha} = \frac{2\pi n}{\pi(n-2)} = 2 + \frac{4}{n-2} (a \in N^+) \tag{3}$$

Hence, n is constrained to be 3, 4, 6. To further filter the support point patterns, the hexagon support point pattern group is analyzed firstly in Fig. 17. The periodic points can be broken down into two equilateral triangle patterns, as shown in Fig. 17(c_1) and (c_2). In essence, the hexagon periodic support point pattern can be seen as two overlapping equilateral triangular patterns. Either of the two equilateral triangular patterns can play a good supporting role on the regular hexagon overhang area. Hence, the periodic support point pattern of equilateral triangle has a better performance than the regular hexagon.

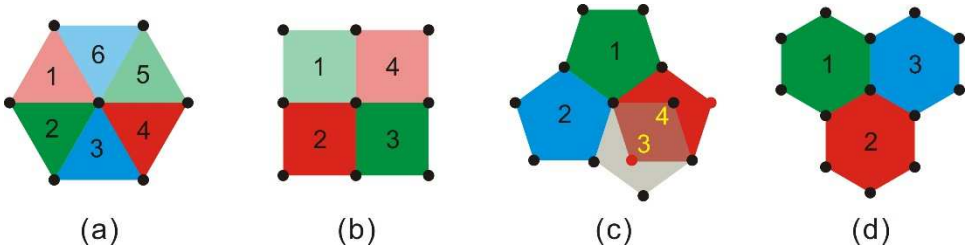

Fig. 16. Periodic support point patterns of multi-group regular polygons: (a). side = 3; (b). side = 4; (c). side = 5; (d). side = 6.

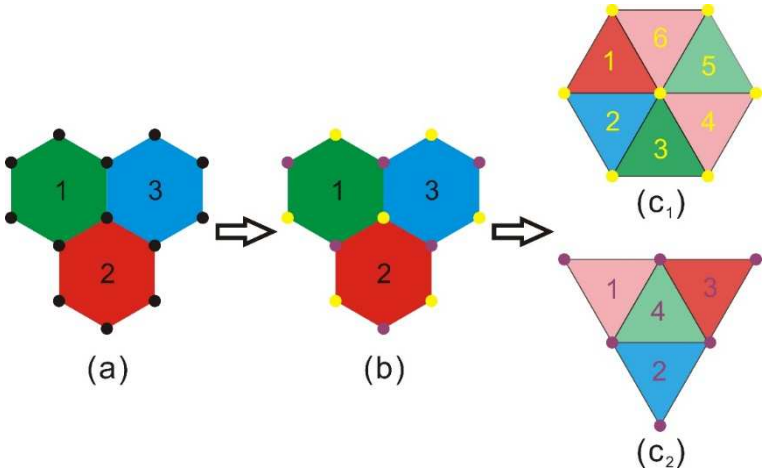

Fig. 17. Periodic support point pattern decomposition of a multi-group regular hexagon pattern.

Fig. 18 gives the comparison between equilateral triangular and regular quadrilateral periodic point patterns. As to an equilateral triangle periodic support point pattern in Fig. 18(a), the area of the overlapping part of two adjacent circles (S_0^3) can be written as:

$$S_0^3=2(\frac{\pi r^2}{6}-\frac{\sqrt{3}r^2}{4}) \tag{4}$$

All overlapping areas for circle *O* in Fig. 18(c) can be measured as $6S_0$ and the ratio (η^3) of the area of the non-overlapping area to circle *O* is:

$$\eta^3=\frac{\pi r^2-6S_0^3}{\pi r^2}=\frac{3\sqrt{3}}{\pi}-1=65.40\% \tag{5}$$

Regarding regular quadrilateral periodic support point pattern, S_0^4 and η^4 can be calculated as:

$$S_0^4=2(\frac{\pi r^2}{4}-\frac{r^2}{2}) \tag{6}$$

$$\eta^4=\frac{\pi r^2-4S_0^4}{\pi r^2}=\frac{4}{\pi}-1=27.32\% \tag{7}$$

In terms of overlapping areas, an equilateral triangle pattern has a better efficiency than a regular quadrilateral pattern on overhang regions.

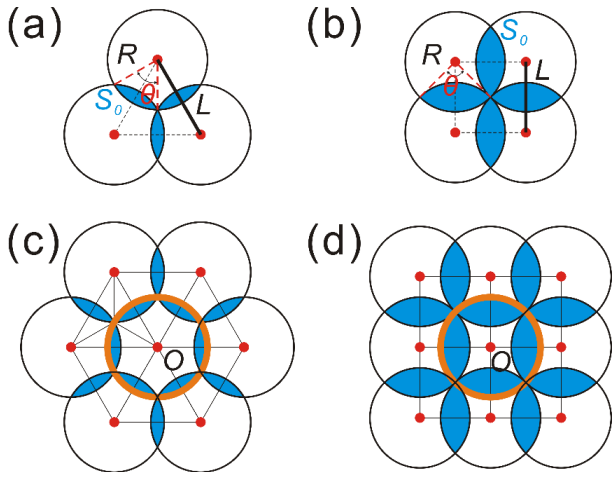

Fig. 18. Comparison of periodic support point patterns: (a) side length $L=\sqrt{3}R$, internal angle $\theta=\pi/3$; (b) side length $L=\sqrt{2}R$, internal angle $\theta=\pi/2$; (c) multi-group support point patterns of equilateral triangle; (d) multi-group support point patterns of regular quadrilateral.

In order to further validate the efficiency of an equilateral triangle support point pattern, a square overhang region is provided to cover support points by using two types of periodic support point patterns (as shown in Fig. 19). The result shows that 941 triangle support points can support the overhang areas, but 1225 quadrilateral support points are needed to support the same region.

$$\eta=\frac{n^4-n^3}{n^3}\times 100\%=30.18\% \tag{8}$$

The triangular point pattern can reduce the support points by at least 30% when compared to the quadrilateral pattern. Therefore, an equilateral triangular periodic support point pattern has a better support performance than a quadrilateral pattern. The former will be applied to optimize support point distribution in the next subsection.

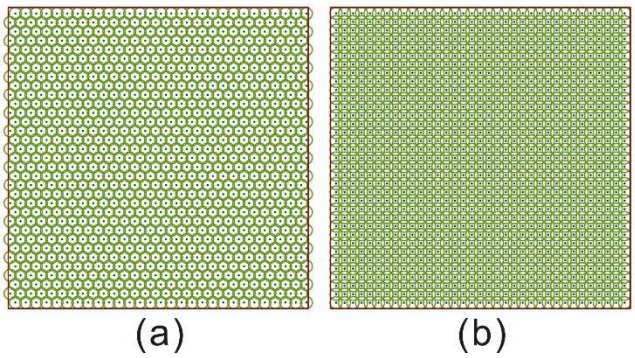

Fig. 19. Two support point distributions for a square overhang region (100 * 100): (a). equilateral triangular pattern (the number of support points = 941); (b). regular quadrilateral pattern (the number of support points = 1225).

5.2. Support point optimization for support relevant overhang areas

Usually, a key goal of support structure design is to minimize the volume of support structures. Many factors can impact the objective, such as the geometric shape of support structure, the number of support points, the position of support points, etc. Among them, generally for the same support structure design method (support shape generation method), the number and position of support points on support relevant overhang areas have a direct influence on the support structure generation. Take the direct projection method as an example, two main factors can influence the support volume, the number and projection lengths of support points (determines the total support volume). Therefore, the aim of support point optimization in the proposed approach is defined to find the most suitable support point distribution, or to minimize the sum of z

coordinate value of support points on the support relevant overhang areas. The objective can accurately reflect the sum of projection length for all support points from the printing base. The objective function can be described below:

$$F(x): min \sum_{i=1}^{n} z_i (i = 1, 2, ..., n) \tag{9}$$

Where z_i is the z value, overhang height at support point P_i $(i = 1, 2, ..., n)$. The constraint is that all support relevant overhang areas should be covered by support point areas. The proposed method uses overhang areas projected onto the XOY plane to optimize the support point distribution. Once overhang areas are projected onto the XOY plane, they are converted into a set of polyline boundary surfaces. Therefore, the projected overhang areas for a non-porous overhang area is a polyline boundary. However, in terms of porous overhang areas, the projected overhang areas are several closed polylines, including outer and inner closed polylines. Notice that the support points should be located in the outer closed outlines and not in the inner polylines. Hence, in this subsection, non-porous and porous overhang areas are discussed, respectively.

5.2.1. Support point optimization for a non-porous overhang region

Fig. 20 describes the workflow of support point generation & optimization on a non-porous overhang area. A re-projection optimization strategy is developed. Here, a non-porous overhang area illustrated in Fig. 21 is discussed in more detail. At first, the overhang area is projected onto the build base, XOY plane. The mesh projection area (Fig. 21(a)) is converted into a closed polyline boundary (Fig. 21(b)). Then, the overhang projection is covered by a set of equilateral-triangular periodic support points in an enlarged bounding box. Fig. 21(c) represents the periodic support point pattern using an equilateral triangle. These points inside the projected region are found to provide support for the overhang area. The support area obtained is shown in Fig. 21(e). However, these support points cannot support all overhang projection areas. A non-supported enlarged area is shown to the left of Fig. 21(e). Fig. 21(f) describes all unsupported overhang areas in green that the triangular point pattern cannot support. In order to support the unsupported overhang regions, supplementary points are generated to provide support for these areas. In addition, small unsupported projected regions will be ignored. Repeat this process until all unsupported areas are supported. The final support region (Fig. 21(h)) is obtained by combining identified equilateral triangular support points and supplementary points on the projected overhang region. Finally, these points within the area are re-projected onto the 3D overhang areas to obtain an alternative solution.

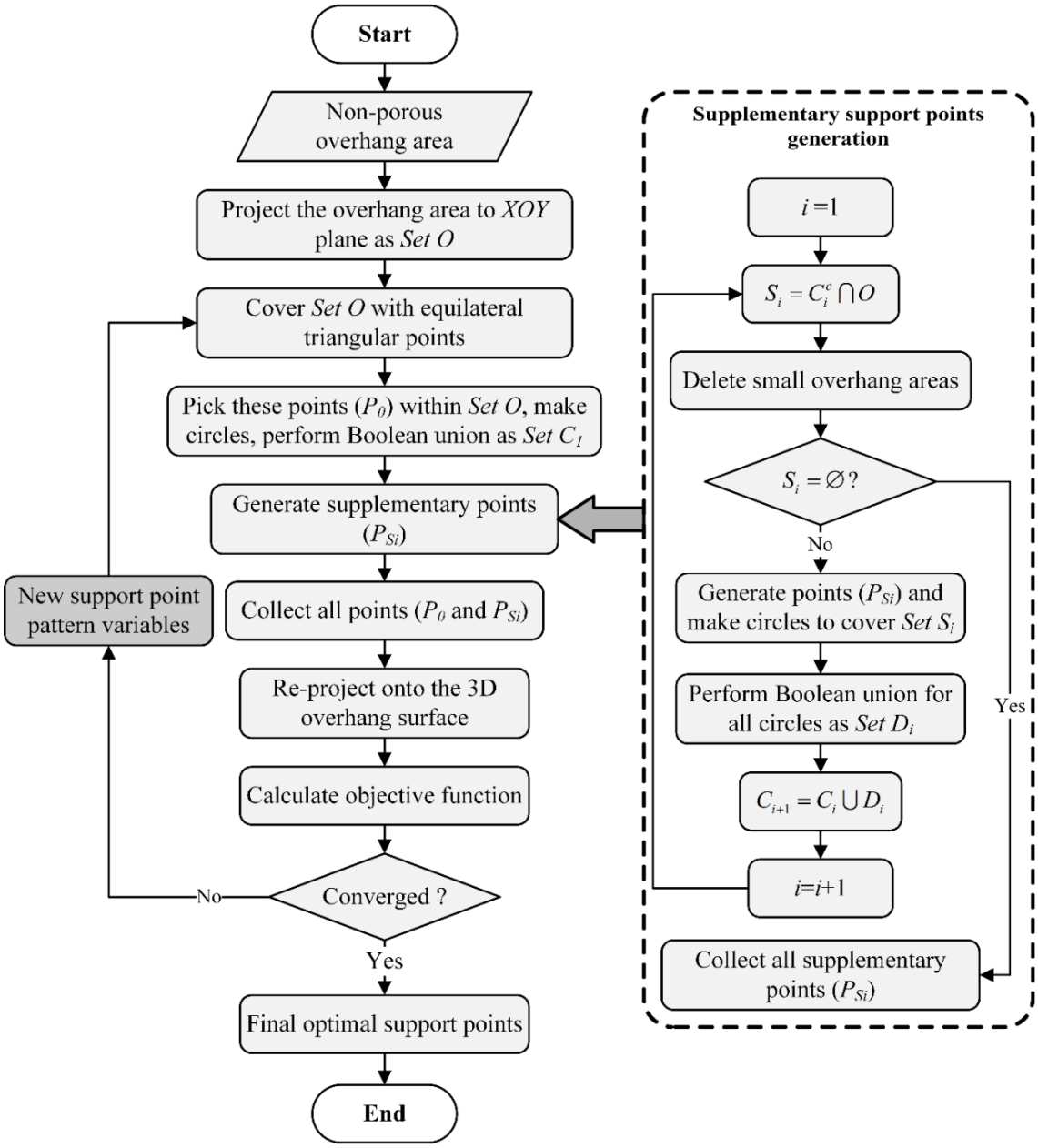

Fig. 20. Workflow of support point generation & optimization on a non-porous overhang area.

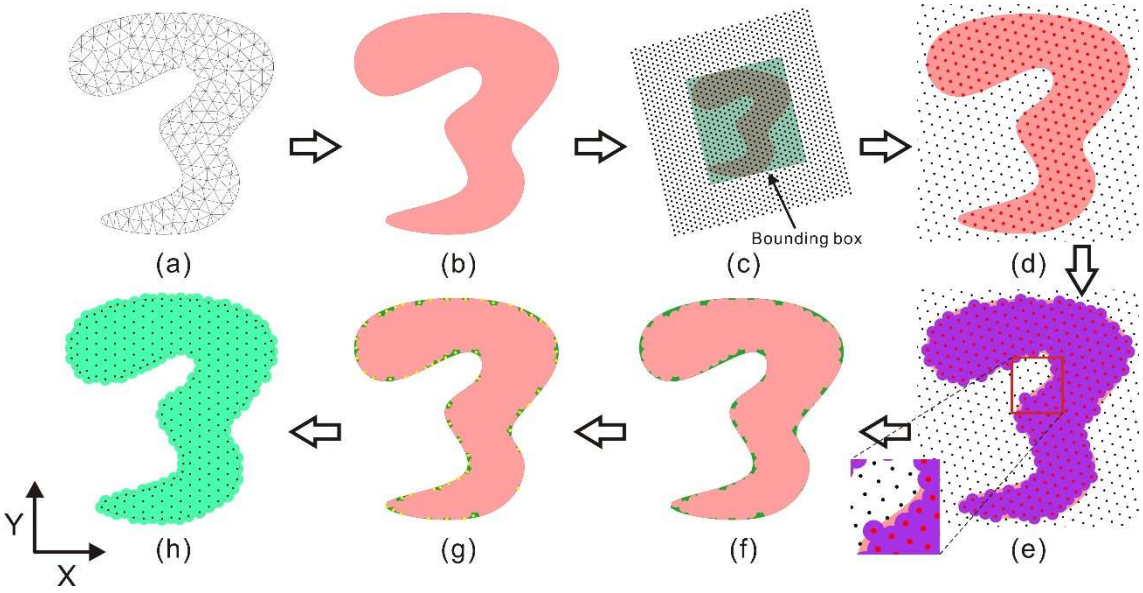

Fig. 21. Equilateral triangular support point pattern for a non-porous structure: (a). overhang mesh projected onto the XY plane; (b). polyline boundary surface; (c). equilateral triangular support points projected onto the overhang regions in the enlarged bounding box; (d). support points in the projected overhang areas; (e). support area that support points inside the overhang areas can support; (f). unsupported areas; (g). supplementary support points on the non-support areas; (h). all support points on the overhang region and support area.

After that, a GA method is applied to search for the optimal triangular point patterns. Taking the support structure design into account, fewer support points are obtained to minimize the volume of support structures. Since the support structure volume has a direct positive correlation with the number and position of support points, the formula (9) is used as the objective function to optimize support point distribution. Two variables, the translation vector and rotation angle of the periodic support point pattern on the XOY plane, are set to populate the alternative solution. The 2D triangular support point pattern can be translated and rotated to achieve the minimal objective function value. It should be noted that the distance between 2 points in the support point pattern should respect the maximum printing bridge length of AM capability to ensure that there is no collapse in printing. Fig. 22 below describes an illustration of the variable definition in support point optimization.

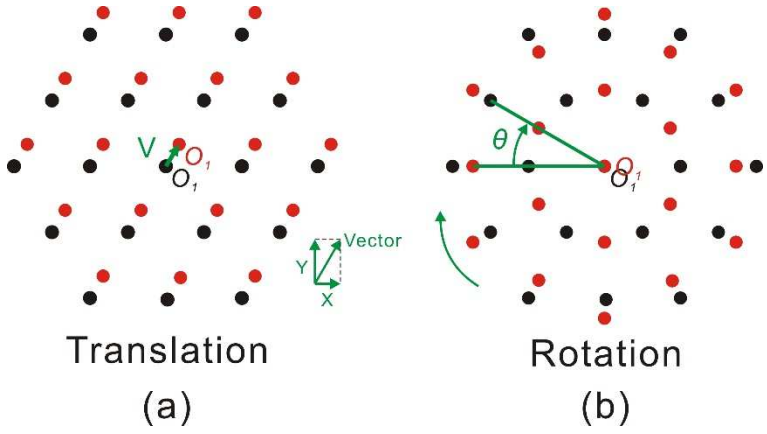

Fig. 22. Two variables defined for the evolutionary algorithm in the support point optimization (original pattern in black): (a). translation vector $\vec{V}$ of the periodic support point pattern; (b). rotation angle θ of the periodic support point pattern.

5.2.2. Support point optimization for a porous overhang region

In terms of a porous overhang region, the overhang area can be divided into two parts, the outer overhang outline and the inner non-overhang areas. It can be noticed that support points should be located inside the outer overhang outline and outside the inner non-overhang areas. Fig. 23 and Fig. 24 below describe the proposed workflow of support point generation & optimization on a porous overhang region. The additional

module of supplementary support point generation is the same as the one used in the non-porous overhang areas above.

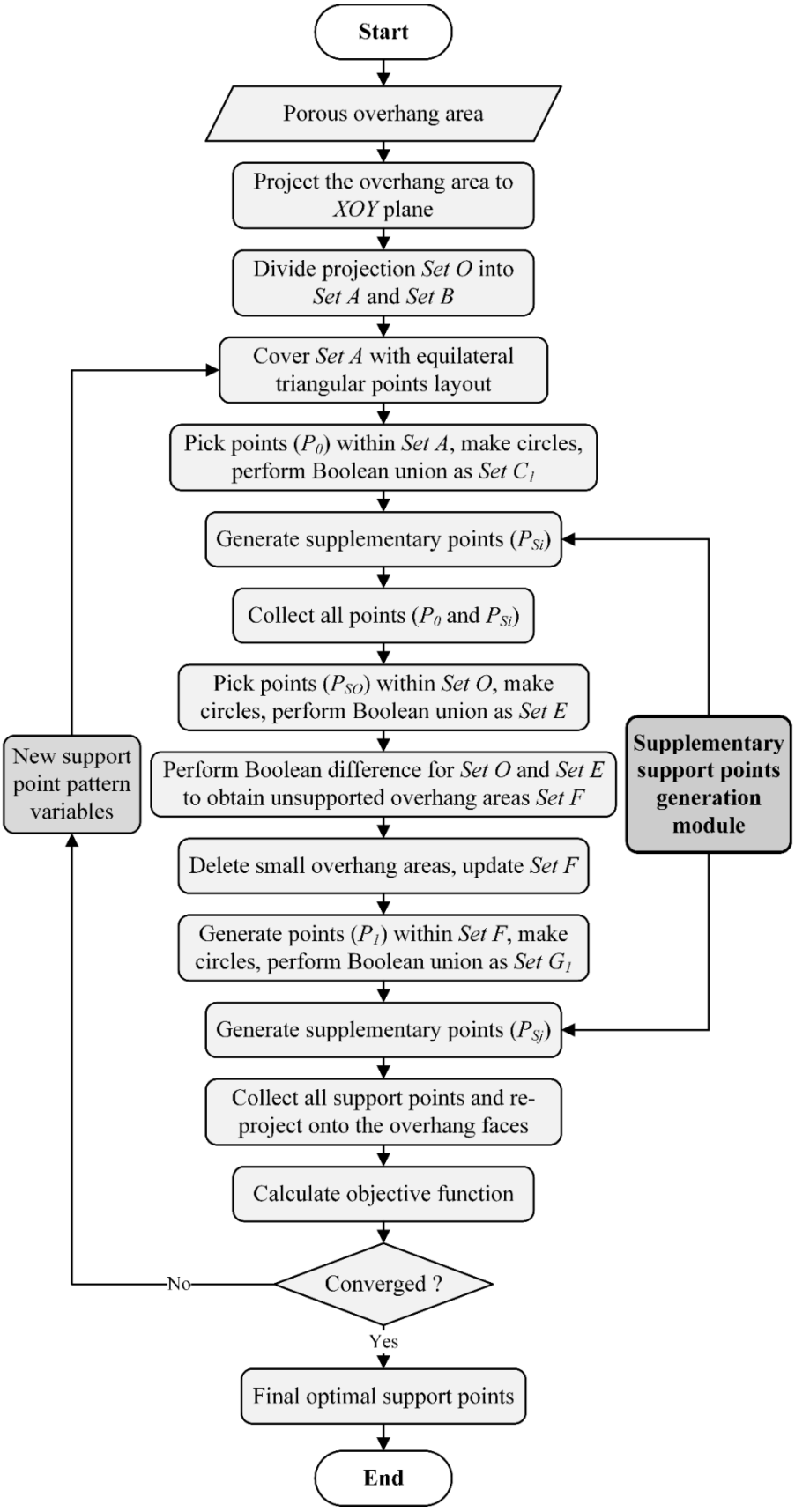

Fig. 23. Flowchart of support point generation & optimization for a porous overhang area.

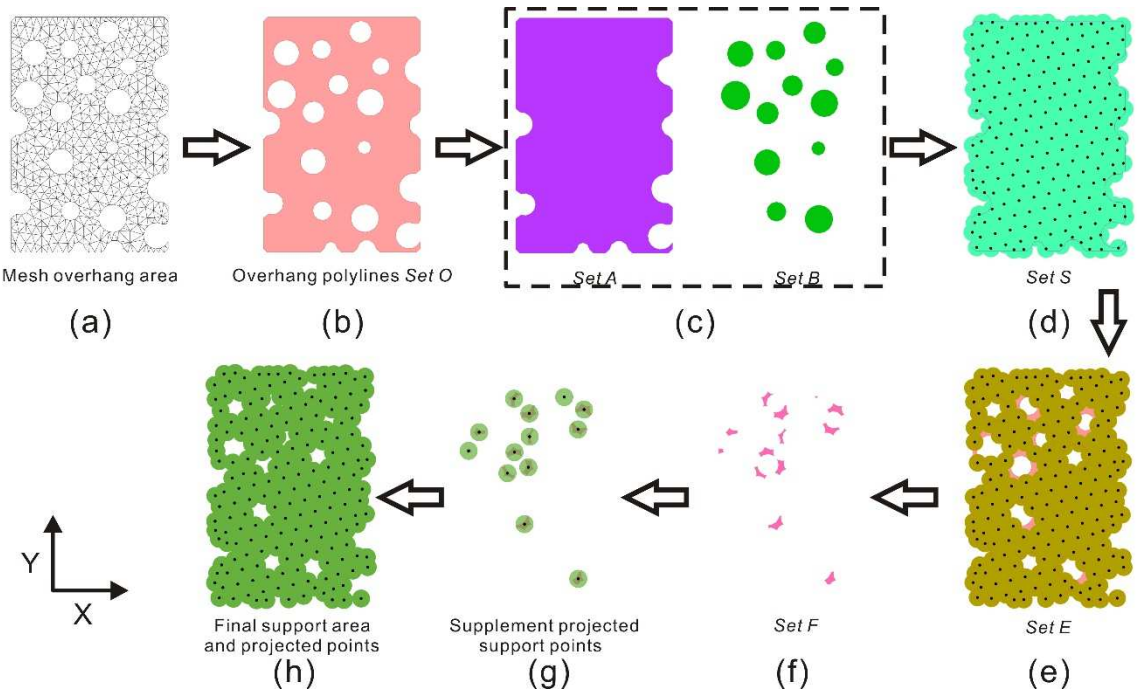

Fig. 24. Workflow of support point generation for a porous overhang area: (a). a support relevant porous overhang area projected; (b). the overhang polylines boundary surface; (c). an outer overhang outline surface (*Set A*) and inner non-overhang areas (*Set B*); (d). apply equilateral triangular periodic point pattern to find all support points on *Set A* and the corresponding support area (*Set S*); (e). the support points on *Set A* are checked to find identified support points on *Set O* and *Set E* is the corresponding support area of the identified support points; (f). identified unsupported areas (*Set F*) after deleting small unsupported areas; (g). all supplementary points on *Set F*; (h). all support points projected and the actual support area.

First of all, a support relevant porous overhang area (Fig. 24(a)) is projected onto the XOY plane and converted into 2D projection polylines area as shown in Fig. 24(b). The projection area can be divided into an outer outline surface (*Set A*) and inner polylines surfaces (*Set B*). Then, the workflow of a non-porous overhang area is applied to cover *Set A* with a 2D projected support point pattern. Fig. 24(d) describes all projected support points on *Set A*. However, only the projection support points located on *Set O* can play a supporting role. Identified projected support points on *Set O* are illustrated in Fig. 24(e) and the corresponding support area is named *Set E*. Red regions represent unsupported areas obtained by performing a Boolean difference operation between *Set O* and *Set E*. After ignoring some small unsupported areas, the actual unsupported areas are presented in Fig. 24(f). To support these unsupported areas, a set of supplementary points are generated onto these areas. Fig. 24(g) displays the supplementary projected support points and the corresponding support areas. At last, the identified equilateral triangular support points and the supplementary points are collected into a support point set. The final support area and projected support points are shown in Fig. 24(h). As with the non-porous overhang area, a GA method is used to obtain the optimal support point distribution.

5.3. Pre-process overhang regions with predefined support points

In medical applications, e.g. printed dental components, it is hard to design fixtures for machining in cutting removing due to the fragile characteristic of the components. Therefore, support structures of these dental component are usually removed manually. In [21], cone tips arranged at support points can achieve the removal of support structures more easily. It is essential to find an optimal support point solution under AM capability while ensuring all support relevant overhang areas supported. Based on the discussions above, support points located in the overhang points and edges need to be supported firstly in order to avoid collapse in the printing process and scraped in the laying powder process. Hence, a pre-processing with predefined support points should be carried out in the specific overhang regions to maintain printing stability. By doing a pre-processing support points selection, a non-porous overhang area with overhang points and edges can be converted into a porous overhang area. A more general workflow for a porous overhang area is shown in Fig. 25. In the workflow, support points on the overhang points and edges can be seen as predefined support points. The support areas covered by the predefined support points are predefined

support areas called *Set X*. The set is combined with *Set B* to act as updated inner non-overhang areas. After that, the support point generation and optimization module is applied to obtain a set of optimal support points. The proposed method has the potential to optimize support point distribution for SLM process and can also be adopted for support structure generation in other AM processes.

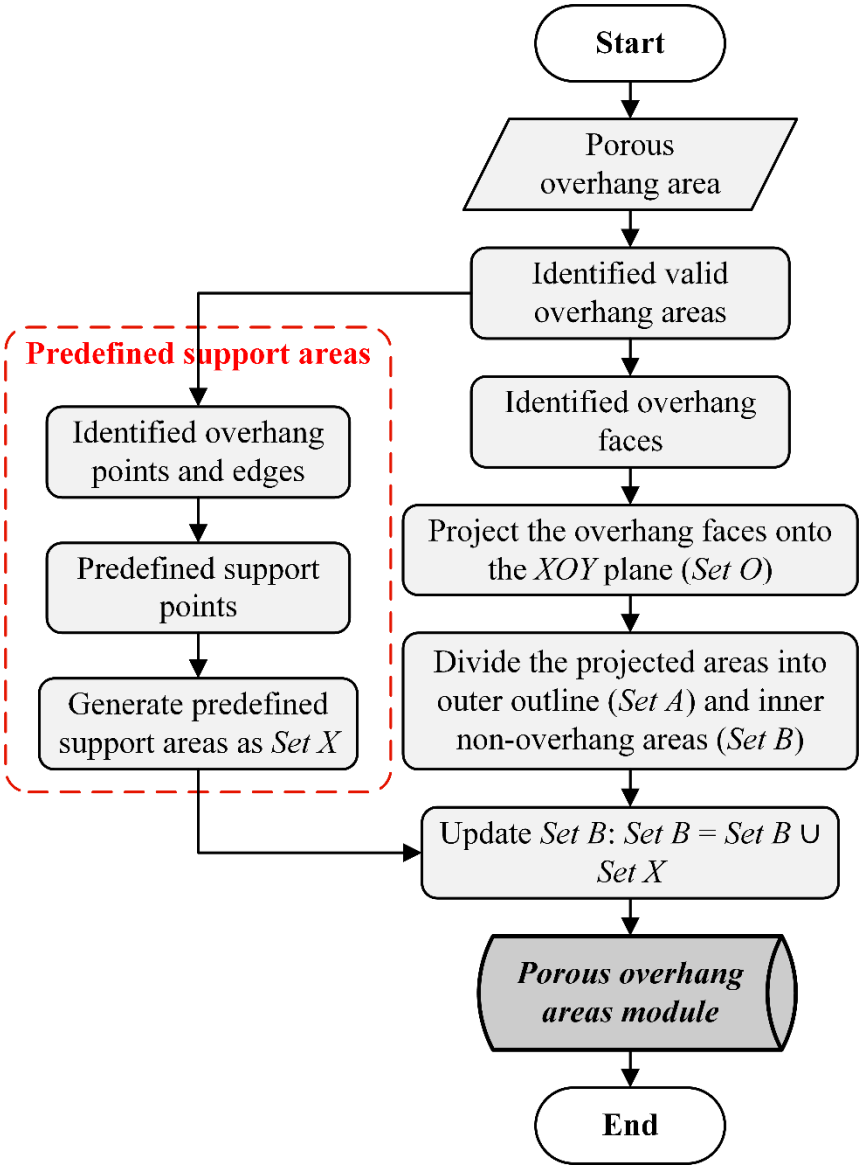

Fig. 25. A general workflow of a porous overhang area with overhang points and edges.

6. Case study and discussion

In this section, a real dental part (Fig. 2) of a patient is selected for a case study to validate the proposed method. The proposed method is validated in an open-source graphical programming tool, Grasshopper, which runs within the Rhinoceros 3D CAD software. As seen above, the edge of the equilateral triangle should respect the maximum radius of a support point under AM capability, maximum printing bridge length and maximum overhang angle, in order to avoid any surface collapse in printing. In this example, the maximum radius of a support point and overhang angle are set as 1 mm and 45°, respectively, to ensure shape accuracy though the SLM machine used can have a maximum printing bridge length of up to 4 mm (for the selected material and adopted processing parameters in this case). Hence, the side length of the equilateral triangular pattern is $\sqrt{3}$ mm.

According to the method above, the first step is to identify and determine support relevant overhang areas. Fig. 26(a) gives the build orientation of the dental part. In terms of overhang points on the overhang edges, a sequence of support point generation is determined as shown in Fig. 26(b). Support points on the support

relevant overhang points and edges are defined as predefined support points. Fig. 26(c) shows the results of all predefined support points. In addition, the support relevant overhang faces are also shown in Fig. 26d). Once all predefined support points are obtained, these support points on the overhang faces are selected to convert the original overhang areas into modified areas.

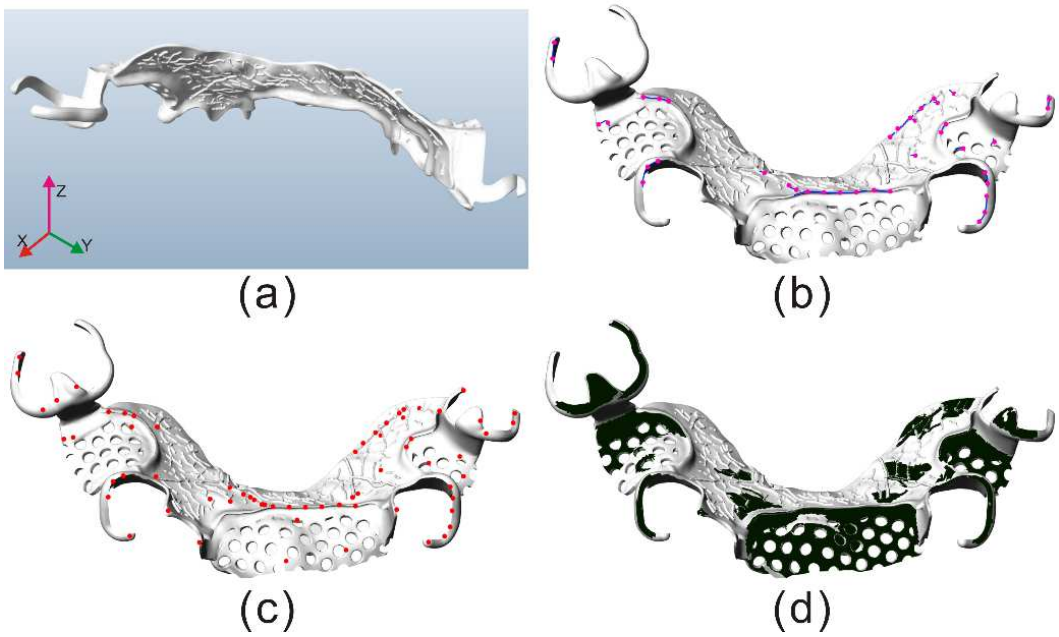

Fig. 26. (a). build orientation (*Z* direction) of the part; (b). support points on the overhang edges; (c). all predefined support points; (d). the support relevant overhang faces.

A porous overhang area in the dental component, as shown in Fig. 27, is introduced to list the support point generation procedure. The porous overhang area is broken down into an outline area in *Set A* and inner non-overhang areas as *Set B*. Moreover, self-supporting overhang areas (*Set C)* are identified by using the method as presented in Fig. 9. Predefined overhang points are shown in *Set P*. Based on the workflows in Fig. 23 and 24, the optimal support points and corresponding support area are presented in Fig. 27(h).

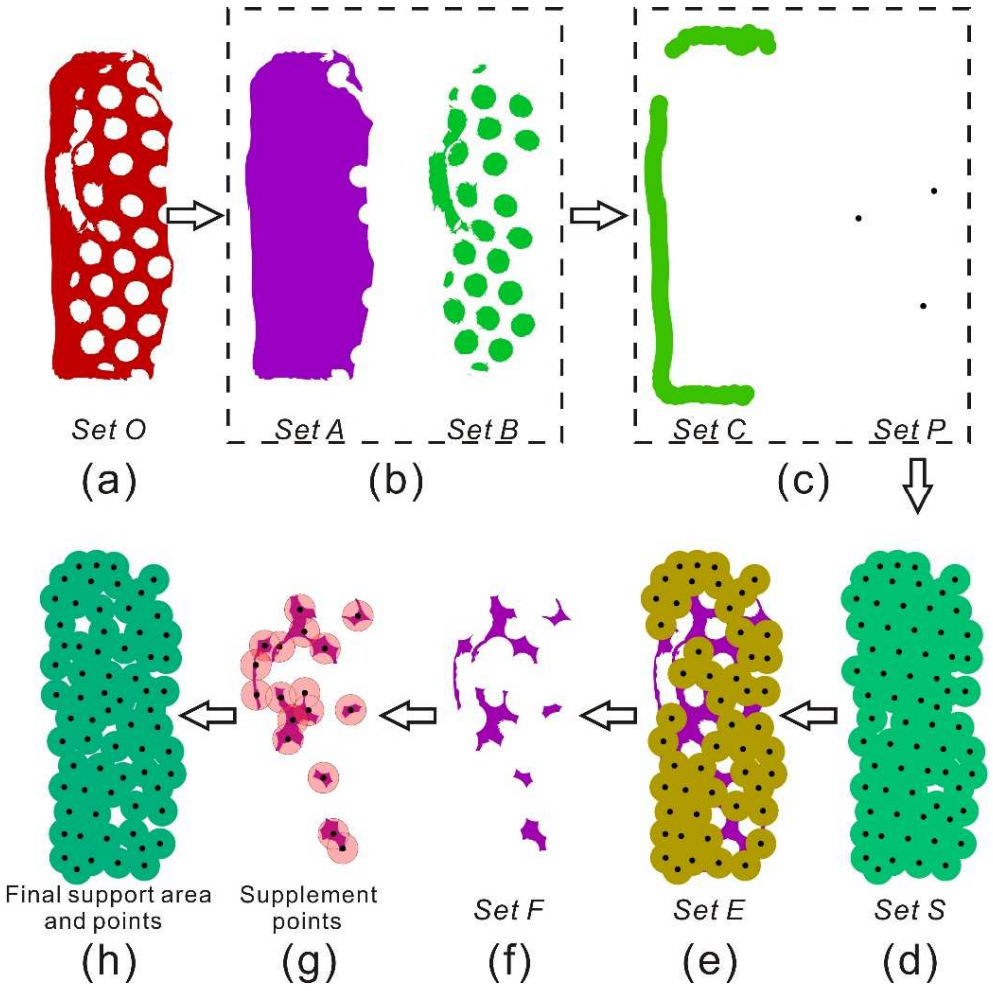

Fig. 27. Support point generation workflow of a porous overhang structure on the dental part (middle bottom section in Fig.26-d): (a). the projected porous overhang area; (b). an outer overhang outline surface (*Set A*) and inner non-overhang surfaces (*Set B*) (c). self-supporting overhang areas (*Set C*) and predefined support points (*Set P*); (d). support points on identified outline overhang areas (*Set S*); (e). support points on the support relevant overhang areas (*Set E*); (f). unsupported areas after deleting small regions (*Set F*); (g). all supplementary points on *Set F*; (h). all support points and actual support area.

A GA method is implemented to search for an optimal solution. Three variables, rotation angle and translation values along x and y directions, are defined to control the distribution of support points on the support relevant overhang area. The Elitist selection and single-point crossover operation are applied to keep the best solution and improve the diversity of population, respectively. A simple random mutation operator is used to prevent the GA converging to a local minimum. The crossover and mutation rates are set as 0.9 and 0.2, respectively. For the support relevant overhang area in Fig. 27, the initial parameters are set as: population size, 20; stop criterion of the optimization, 100 generations. The run will end when the maximum number of generations is obtained. Parameters in the GA are defined in Table 2. The fitness function is to minimize the sum of z coordinate value of support points as illustrated in the Eq. 9. Evaluation of the fitness function value of the best creature at each iteration is shown in Fig. 28. In the optimization procedure, it is clear that as the numbers of support points decrease, the total support length, representing resulted volume for the projection-based support design method, reduces.

Table 2. Parameter definition of the GA.

Option	Description
Crossover probability	0.9
Mutation probability	0.2
Population size	20
Generations	100

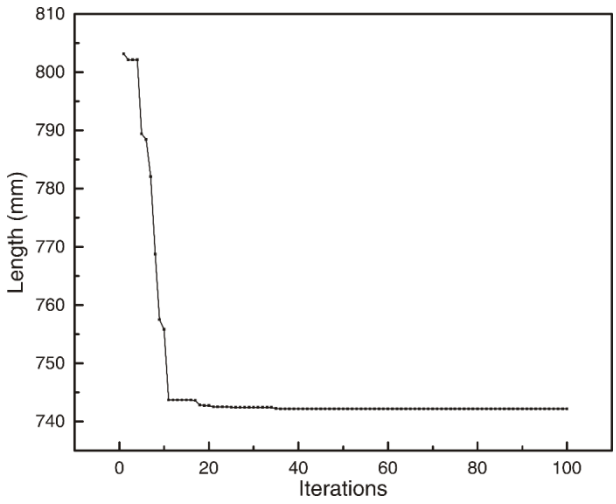

Fig. 28. Convergence curve of the optimization.

Due to the huge difference in shape and distribution of the overhang faces on the part, it is hard to obtain an optimal support point distribution by populating a varying periodic point pattern on all support relevant overhang faces. Therefore, the identified overhang faces are divided into different groups. The final optimal support points on the support relevant overhang areas are presented in Fig. 29.

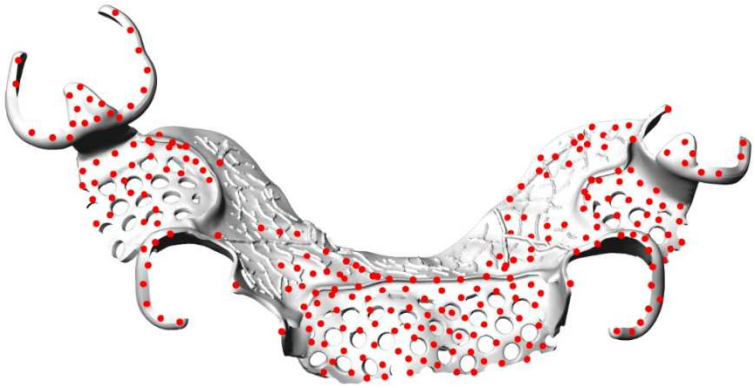

Fig. 29. All 249 support points on the support relevant overhang areas.

The proposed method has two main objectives: one is to decrease the number of points for reducing the total support structure volume and the number of support contact points for post-processing. The other objective is that the obtained optimized support points can be used as input for different support generation/design methods to generate lightweight but solid support structures to ensure printing quality, usually including surface roughness and shape accuracy. To show the effectiveness of this method, a dental part is processed, first, by using one of the representative commercial tools, Netfabb, and the proposed method to compare the number of support points/contact points. Fig. 30 shows the support point result obtained by using Netfabb. The same critical overhang distance constraint is utilized to obtain the support point result. The minimal area threshold is set as 0.1 mm. Compared with the proposed method, the number of support points through Netfabb is 291 (Note: support structure was exported into an in-house developed code to detection of the number of contact points).

As shown in the Fig. 30, the proposed method has a less number of support points, which means this will usually result in a less support volumes in total when using the same support generation/design method. In addition, the proposed method can ensure that all support relevant overhang areas are supported, while Netfabb will delete small support relevant overhang areas. Hence, it is expected that other support design method can also adopt this support point optimization method to reduce support point numbers and therefore support volumes with ensured manufacturability. However, most of the popular commercial printing preparation software tools are not open source and cannot accept optimized support point set generated by the proposed method as input to generate support structures via their own specific support design methods

for further comparison. This case study here only shows the difference on number of support points between the proposed methods and that of the commercial tool. Intuitively, reduced support points may cause reduced total contact area but have better surface protection, and save more support volume as discussed above.

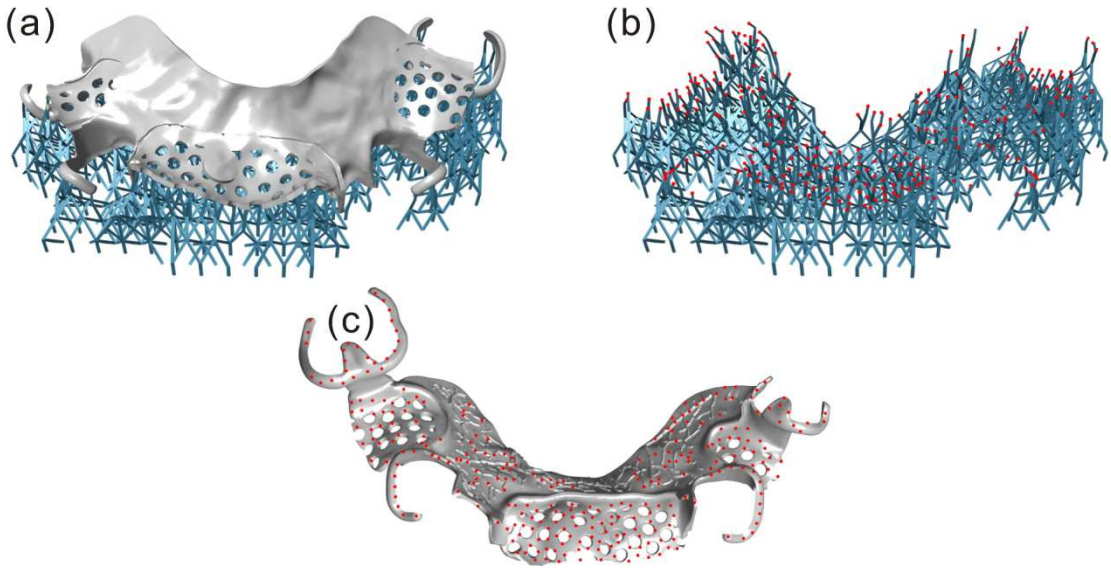

Fig. 30. Support structure and support points obtained by using Netfabb: (a). the dental part with support structures; (b). lattice support structures with support points; (c). support points projected on the part.

To demonstrate the effectiveness for the second objective, the optimized support points of the dental part are used as input in two different support generation methods (in-house codes): the direct cone method (also used by many commercial software tools) and a bio-inspired tree-shaped structure design method (an academic tool) [21], to check whether the printing quality can be achieved. A Ti-6Al-4V powder material and a Profeta SLM medical fabrication machine [27] with an existing recommended industrial working parameter setting are used for printing. A heat treatment is applied to relief the thermal stress. The temperature of the stress relief annealing treatment is set as 820°C keeping for 2 hours and cooling with the furnace. Fig. 31(a, b) gives the results of a printing experiment, where two copies of the case part with the same set of support points but different support structures are printed successfully without any collapse. This means the two different support structures have sufficient support strength. Then, after removing the support structures and conducting other simple post-processing steps (e.g. sanding), the two printed parts are measured by a scanner to generate two 3D surface deviation maps for quality evaluation. According to the shape accuracy requirement of the dental part, the standard deviation of a surface should be estimated to be ± 0.2 mm. In Fig. 31(c, d), main distortions occur on porous regions with many holes. The deformation in those regions are within ± 0.2 mm, which means that the final parts after post-processing can meet the dimensional accuracy requirement. Therefore, as expected, the optimized support point set used in the two support design methods can generate qualified support structures to ensure manufacturability and achieve printing quality.

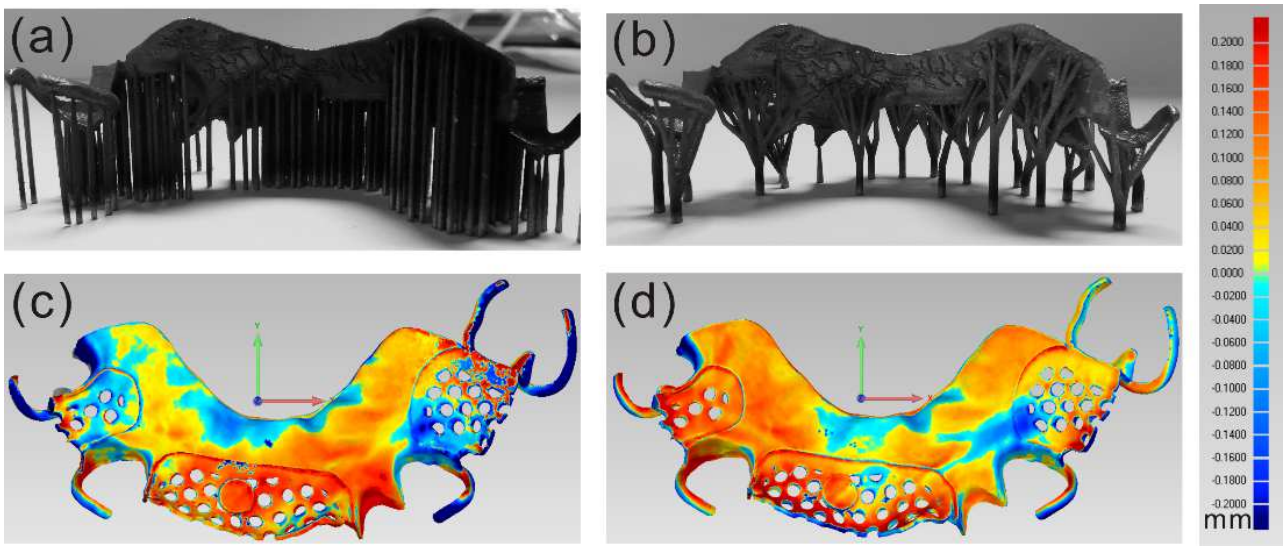

Fig. 31. Printed examples with the supports from two support structures. (a). the direct cone support; (b). a bio-inspired tree-shaped support [21]; (c). a 3D surface deviation map after removing support structures for the cone support; (d). a 3D surface deviation map after removing supports for the tree-shaped support.

In general, the case study shows that the proposed method can improve the support design preparation for the SLM process. Although extensive testing and quantitative comparison with other commercial tools is difficult since many AM preparation software tools are not open source as said above and it is hard to directly control the input of assigned support points, the proposed method has the potential of being able to be applied in different AM preparation software tools as an integrated function for support design. The printing experiment example above, where the two in-house support design methods were applied, already proved this feasibility. Hence, it can also be applied to other AM processes where support design is necessary. For other specific AM processes, specific manufacturing constraints should be considered and integrated into the proposed support point optimization process, which means adaptation is necessary.

7. Conclusion and future challenges

This paper proposes a support point optimization method to detect support relevant overhang areas and generate optimal support points on the overhang areas of complex components in AM. Point, edge and face overhangs are discussed, respectively, to determine the sequence of generating support points. Taking into account the maximum printing bridge length of AM capability, the predefined support points are discussed and a new equilateral-triangle periodic support point pattern is proposed to optimize the support point distribution on the support relevant overhang areas. For a regular rectangular overhang area, the proposed support point pattern can decrease the number of support points by 30%. Hence, the method has potential to be applied to more types of support structure generation. A general optimization method is implemented to optimize the support point distribution while ensuring that all types of support relevant overhang areas can be supported, especially those from complex and porous components.

In summary, the proposed support point optimization method has obvious advantages in reducing unnecessary support points while ensuring manufacturability as shown by the case study. It may be used with existing support structure design methods to further reduce the support volume, improve the surface quality and decrease the post-processing time. Hence, it can be developed as a key function for printing preparation software tools in industry.

However, there is still space for improvement in the proposed method. Firstly, the heat diffusion and thermal stress deformation should be considered in the support point generation for large size metallic components. One solution is to conduct the thermal stress by predefined support points where the thermal stress is too large. Secondly, a part of the face overhang areas can be supported by the local non-supported areas, called self-support caused by maximum printing bridge length. Hence, how to simplify the support relevant face overhang areas still plays a key role in the support point generation. In addition, the slicing method could

provide a better solution for detecting the support relevant overhang areas. Support point distribution is one of the key factors that impact shape accuracy. To further demonstrate the support point optimization method, different types of support structures can be populated under support points with different positions. These are the necessary investigations for further research.

Acknowledgements

This research work has benefited from financial support of China Scholarship Council (first author), under Grant No. 201806950079. The authors also would like to thank Nanjing Profeta Intelligent Tech. Co. for their support on providing dental models and AM process parameters for case study experiments.

References

[1] T. Vaneker, A. Bernard, G. Moroni, I. Gibson, Y. Zhang, Design for additive manufacturing: Framework and methodology, CIRP Annals 69(2) (2020) 578-599.
[2] M.K. Thompson, G. Moroni, T. Vaneker, G. Fadel, R.I. Campbell, I. Gibson, A. Bernard, J. Schulz, P. Graf, B. Ahuja, F. Martina, Design for Additive Manufacturing: Trends, opportunities, considerations, and constraints, CIRP Annals 65(2) (2016) 737-760.
[3] N. Lebaal, Y. Zhang, F. Demoly, S. Roth, S. Gomes, A. Bernard, Optimised lattice structure configuration for additive manufacturing, CIRP Annals 69(1) (2019) 117-120.
[4] Y. Zhang, A. Bernard, R. Harik, K.P. Karunakaran, Build orientation optimization for multi-part production in additive manufacturing, Journal of Intelligent Manufacturing 28(6) (2015) 1393-1407.
[5] Y. Zhang, W. De Backer, R. Harik, A. Bernard, Build Orientation Determination for Multi-material Deposition Additive Manufacturing with Continuous Fibers, Procedia CIRP 50 (2016) 414-419.
[6] A. Hussein, L. Hao, C. Yan, R. Everson, P. Young, Advanced lattice support structures for metal additive manufacturing, Journal of Materials Processing Technology 213(7) (2013) 1019-1026.
[7] S. Kapil, P. Joshi, H.V. Yagani, D. Rana, P.M. Kulkarni, R. Kumar, K.P. Karunakaran, Optimal space filling for additive manufacturing, Rapid Prototyping Journal 22(4) (2016) 660-675.
[8] K. Zeng, D. Pal, C. Teng, B.E. Stucker, Evaluations of effective thermal conductivity of support structures in selective laser melting, Additive Manufacturing 6 (2015) 67-73.
[9] M. Cloots, A. Spierings, K. Wegener, Assessing new support minimizing strategies for the additive manufacturing technology SLM, 24th International SFF Symposium-An Additive Manufacturing Conference, Austin, USA, University of Texas at Austin, 2013, pp. 631-643.
[10] J.L. Bartlett, X. Li, An overview of residual stresses in metal powder bed fusion, Additive Manufacturing 27 (2019) 131-149.
[11] G. Strano, L. Hao, R.M. Everson, K.E. Evans, A new approach to the design and optimisation of support structures in additive manufacturing, The International Journal of Advanced Manufacturing Technology 66(9-12) (2012) 1247-1254.
[12] M.X. Gan, C.H. Wong, Practical support structures for selective laser melting, Journal of Materials Processing Technology 238 (2016) 474-484.
[13] R. Vaidya, S. Anand, Optimum Support Structure Generation for Additive Manufacturing Using Unit Cell Structures and Support Removal Constraint, Procedia Manufacturing 5 (2016) 1043-1059.
[14] B. Vaissier, J.-P. Pernot, L. Chougrani, P. Véron, Genetic-algorithm based framework for lattice support structure optimization in additive manufacturing, Computer-Aided Design 110 (2019) 11-23.
[15] R. Schmidt, N. Umetani, Branching support structures for 3D printing, ACM SIGGRAPH 2014 Studio2014, pp. 1-1.
[16] J. Vanek, J.A.G. Galicia, B. Benes, Clever Support: Efficient Support Structure Generation for Digital Fabrication, Computer Graphics Forum 33(5) (2014) 117-125.
[17] N. Zhang, L.-C. Zhang, Y. Chen, Y.-S. Shi, Local Barycenter Based Efficient Tree-Support Generation for 3D Printing, Computer-Aided Design 115 (2019) 277-292.
[18] L. Zhu, R. Feng, X. Li, J. Xi, X. Wei, Design of lightweight tree-shaped internal support structures for 3D printed shell models, Rapid Prototyping Journal 25(9) (2019) 1552-1564.
[19] L. Zhu, R. Feng, X. Li, J. Xi, X. Wei, A Tree-Shaped Support Structure for Additive Manufacturing Generated by Using a Hybrid of Particle Swarm Optimization and Greedy Algorithm, Journal of Computing and Information Science in Engineering 19(4) (2019).
[20] J. Dumas, J. Hergel, S. Lefebvre, Bridging the gap: Automated steady scaffoldings for 3d printing, ACM Transactions on Graphics (TOG) 33(4) (2014) 1-10.
[21] Y. Zhang, Z. Wang, Y. Zhang, S. Gomes, A. Bernard, Bio-inspired generative design for support structure generation and optimization in Additive Manufacturing (AM), CIRP Annals 69(1) (2020) 117-120.
[22] Materialise e-Stage. https://www.materialise.com/en/software/magics/e-stage.

[23] Autodesk Netfabb. https://www.autodesk.com/products/netfabb/overview.
[24] Y. Zhang, R. Harik, G. Fadel, A. Bernard, A statistical method for build orientation determination in additive manufacturing, Rapid Prototyping Journal (2018).
[25] L. Cheng, A. To, Part-scale build orientation optimization for minimizing residual stress and support volume for metal additive manufacturing: Theory and experimental validation, Computer-Aided Design 113 (2019) 1-23.
[26] D. Thomas, A deep dive into metal 3D printing, Laser 3D Manufacturing VI, International Society for Optics and Photonics, 2019.
[27] Profeta. http://www.profeta.cn/.